A Lagrangian Characterization of the Sources and Chemical Transformation of Air Influencing the US and Europe during the 2004 ICARTT/INTEX-A Campaign

Jassim A. Al-Saadi[1], R. Bradley Pierce[1], T. Duncan Fairlie[1], Todd K. Schaack[2], Melody A. Avery[1], Chieko Kittaka[3], James J. Szykman[4], Tom H. Zapotocny[2], and Donald R. Johnson[2]

[1] NASA Langley Research Center, Hampton, Virginia

[2] SSEC/CIMSS, University of Wisconsin, Madison, WI

[3] SAIC, Hampton, Virginia

[4] US EPA, ORD, Research Triangle Park, NC (currently on assignment to NASA Langley Research Center, Hampton, VA)

Abstract

We apply a novel technique for establishing source/receptor relationships to characterize the dominant contributions to O3 distributions over the continental United States and Europe during the summer 2004 INTEX-A and ICARTT integrated atmospheric field campaigns. In our approach Lagrangian trajectories are used to sample Eulerian fields from the global RAQMS model to establish source/receptor relationships based on geographic, chemical and meteorological criteria. In this way the trajectories provide information on both airmass origins and transformations in chemical composition. We focus on understanding the processes by which long-range transport impacts regional air quality associated with ozone by considering the origins, chemical composition, and chemical transformation of air influencing the United States and Europe. For both regions we find that (1) approximately half the air in the lower troposphere experiences O3 production within the domain upon exposure to local precursor emissions, (2) air influenced by the stratosphere and by strong mixing has origins primarily over the Pacific Ocean 10 days earlier, and (3) exposure to high levels of PAN in the mid-tropospheric characterizes 20-25% of all free tropospheric air. The largest differences between CONUS and Europe are associated with persistent deep convection over the Gulf of Mexico and southern U.S. For CONUS, the Gulf convection is a center of action in which influences from long-range transport, local precursor emissions (anthropogenic and lightning), and regional photochemistry are linked. Within the contexts of INTEX and ICARTT we find relatively little direct Asian influence on ozone over the U.S. during the summer of 2004 (2%) but a sizeable U.S. influence on Europe (9%). We have additionally identified a strong convective coupling between long-range pollution transport and ozone in the U.S. boundary layer.

Introduction

The INTEX-A field experiment was an integrated atmospheric field campaign that took place over North America during summer 2004. Its objectives were to understand the transport and transformation of gases and aerosols on transcontinental/intercontinental scales and their impact on air quality and climate [Singh et al., this issue]. A particular focus was to quantify and characterize the inflow and outflow of ozone, aerosols and their precursors over North America during summer when photochemistry is most intense. INTEX-A was coordinated with field activities conducted by other national and international partners within the International Consortium for Atmospheric Research on Transport and Transformation (ICARTT) to more completely characterize these processes over the North Atlantic and Europe.

The Real-time Air Quality Modeling System (RAQMS) was one of several models used to provide dynamical and chemical forecast guidance for flight planning during the campaign [Pierce et al., this issue]. RAQMS is a global meteorological forecast model of the troposphere and stratosphere formulated in a hybrid isentropic vertical coordinate system well suited for accurate representation of long-range transport. RAQMS includes a unified troposphere/stratosphere chemical prediction scheme focused on processes relevant to ozone formation and destruction and also assimilates satellite O3 observations to better predict the global O3 distribution. Pierce et al. [this issue] fully evaluate the fidelity of the RAQMS simulation for the INTEX-A time period and focus on O3 and NOy budgets over the U.S. This paper focuses on characterizing the large-scale transport and photochemistry that determines the coupling between regional chemical budgets and the global atmosphere. The motivation for this study is to better understand the processes by which long-range transport impacts regional air quality associated with ozone. The importance of this association is reflected by the 1999

adoption of a protocol to abate ground level ozone within the International Convention on Long-Range Transboundary Air Pollution (LRTAP) [United Nations, 2004]. Our specific objective is to quantify the primary factors controlling the ozone budgets of the continental United States (CONUS) and Europe by considering the origins, chemical composition, and chemical transformation of air influencing those regions.

The distribution of ozone in the troposphere is controlled by a combination of photochemistry (local production and destruction) and transport (horizontal and vertical). Figure 1 illustrates these characteristics over the Northern hemisphere (equator to 70N) using results from RAQMS during the INTEX-A time period. Shown are the mean O3 in the boundary layer, mean O3 production in the boundary layer, mean O3 in the upper free troposphere (averaged between 7 km and the tropopause), and mean tropospheric convective mass flux. Boundary layer O3 production is associated with precursor source emissions over continental regions and in particular near populous and industrialized areas, while O3 destruction is found over oceans and unindustrialized areas (e.g., Africa and much of Central America). While highest boundary layer O3 concentrations are found near these regions of strong production, high concentrations also extend away from these regions such as over the oceans to the east of the United States and east Asia. In the upper free troposphere there is a latitudinal gradient in O3 with concentrations increasing from the equator to high latitudes. Strong convective mass flux is an efficient mechanism for rapid vertical mixing of lower and upper tropospheric air. It can be seen in Figure 1 that regions of strong maritime convection are generally associated with local minima in upper tropospheric O3, reflecting the convective detrainment of marine boundary layer air with low ozone mixing ratios into the upper troposphere.

While an Eulerian model such as RAQMS can realistically represent the physical processes controlling the production and transport of O3, including convection and mixing, it is difficult to quantify specific contributions of remote source regions and previous chemical processing to the O3 budget of a particular region. Such a source apportionment capability is necessary for conducting air quality assessment and attribution studies. Apportionment and attribution for O3 are further complicated by the need to consider chemical transformation because O3 is produced from other chemical precursors. Source apportionment approaches that have been employed in both Eulerian and Lagrangian frameworks include the use of tagged tracers (e.g., separately tracking emissions from different geographic regions and source types) and emissions separation techniques (the conduct of multiple simulations in which emissions are systematically varied in order to assess relative contributions). Lagrangian techniques based on tagged tracers are particularly useful for simultaneous consideration of many distinct source types and regions and for assessing relative ages of associated airmasses [Stohl et al., 2002, 2003; Trickl et al., 2003; Holzer et al., 2005]. The use of tagged tracers in Eulerian models includes both local assessments within regional domains [e.g., Fast et al., 2002] and regional assessments within global domains [e.g., Pfister et al., 2004]. Emissions separation techniques are often used to assess emission abatement strategies and to isolate contributions from specific regions or source classes (e.g., anthropogenic, biogenic) [Tao et al., 2003; Li et al., 2004]. Also, combinations of these techniques are often used. Emissions sensitivity studies have been combined with tagged tracers by Fiore et al. [2002] to assess the contributions to background O3 over the U.S. and by Li et al. [2002] to assess the influence of transatlantic pollution transport on European and North American surface O3. Weiss-Penzias et al. [2004] compare source/receptor results from Eulerian and Lagrangian techniques in assessing annual cycles of the long-range transport of CO and O3.

In the present work we consider a hybrid approach in which Lagrangian trajectories are used to sample Eulerian fields from a 3-D model to establish source/receptor relationships based on geographic, chemical and meteorological criteria. By sampling the RAQMS chemical and dynamical fields, the trajectories provide information on airmass origins as well as transformations in chemical composition.

The Lagrangian source/receptor analysis is described in the next section. Next we discuss the results of our analysis for the two large-scale receptor regions considered in ICARTT, CONUS and Europe. Conclusions are drawn in a final section.

Approach

Our Lagrangian source/receptor technique employs a Reverse Domain Filling (RDF) analysis [Sutton et al., 1994] followed by a cluster analysis to establish source/receptor relationships. RDF consists of conducting back trajectory calculations initialized on a grid covering a particular domain of interest, then mapping atmospheric characteristics sampled by the back trajectories onto the initial grid. In our approach RDF is applied to meteorological and chemical fields archived from the RAQMS global INTEX-A simulation, which are available at a 6-hour frequency (00Z, 06Z, 12Z, 18Z) from July 1 through August 15 2004.

For the RDF phase we conduct a series of 10-day back trajectory simulations with trajectories initialized on a uniform Northern Hemisphere grid of 2x2 degrees in the horizontal and on the RAQMS vertical levels from the surface to the lower stratosphere. The trajectories are driven by instantaneous RAQMS 3-D wind fields. The 6-hourly RAQMS chemical/dynamical fields are sampled along each trajectory to accumulate Lagrangian mean quantities. These Lagrangian averages are then mapped back onto the original grid to characterize the chemical/dynamical history of air arriving at each location. A 10-day back trajectory simulation

is initialized at each 6-hourly period from July 11 to August 15 for a total of 144 (36 days, 4 times per day) trajectory simulations.

The cluster analysis starts with classification of unique chemical/dynamical characteristics of air parcels within the receptor regions (e.g., CONUS, Europe). Temporal and spatial composites of the Lagrangian averaged quantities are analyzed to identify these distinct characteristics. Characteristics that we focus on include O3 net photochemical production and destruction, stratospheric influence, convective influence, exposure to selected precursors, and long-range transport from other regions. The characteristics are then used to construct sets of selection criteria against which all back trajectories are evaluated for classification of airmass type. Each set of selection criteria thereby provides a filtered subset of trajectories that uniquely identify the origins of air exhibiting these characteristics. We then analyze the three-dimensional distributions of these parcel origins using geospatial probability distributions to identify the dominant source regions of the receptor airmass classes.

A subtlety of this technique concerns the representation of sub-gridscale processes such as convection and diffusion. Such parameterizations are not directly applied in the trajectory calculations, but the Eulerian fields sampled by the trajectories have been exposed to them. In our Lagrangian framework these influences on airmass composition are accounted for by sampling relevant quantities along the back trajectories. Convective influences are assessed by considering convective mass fluxes and O3 convective mixing tendencies. Diffusive mixing is assessed by considering mixing efficiencies based on large-scale shear deformation [Fairlie et al., 1999]. This approach differs significantly from previous Lagrangian analyses, which include parameterized convective and turbulent dispersion into the trajectory calculations. By accounting for the Lagrangian mean influences of mixing on parcel chemical properties we in effect allow

parcel identities to change, while previous approaches would maintain parcel identity but allow sub-gridscale processes to change parcel positions.

Results

First we examine Lagrangian mean dynamical and chemical quantities (i.e., analysis of the RDF products) to identify dominant features that influence O3 within the receptor regions. These features guide the creation of airmass-based trajectory selection criteria. We consider mean 10-day Lagrangian histories by temporally averaging the Lagrangian means over the entire study period. Hemispheric maps are analyzed to provide a large-scale horizontal perspective and then zonally averaged cross sections within the domains of the two receptor regions are analyzed to refine the selection criteria. Following the hemispheric analysis the results of source/receptor analyses are presented first for CONUS and then for Europe. Note that we use the same categories of selection criteria for both receptor regions except as detailed below.

Lagrangian Mean Maps

Shown in Figure 2 are Northern hemisphere maps of Lagrangian mean tropospheric convective mass flux, stratospheric influence, and boundary layer influence. These maps consist of pressure-weighted means between the surface and the tropopause of the Lagrangian averaged quanities mapped back to the original (uniform) initialization grid. Comparison of the convective mass fluxes shown in Figure 1(d) and Figure 2(a) illustrates the different perspectives offered by the instantaneous (Eulerian) and Lagrangian means. Both quantities show that peak convection occurs over the Gulf of Mexico/Caribbean and tropical western Pacific. The Lagrangian mean is smoother and has maxima that extend over larger areas while the mean instantaneous mass flux is more discrete and has larger maximum values. The Lagrangian mean shows that very large

regions of air have experienced convection at some time during the preceding 10 days, while the Eulerian mean shows the actual regions in which convection is occurring.

Lagrangian mean stratospheric and boundary layer influence are determined by selecting those back trajectories that are initialized in the free troposphere but have been in the stratosphere or boundary layer, respectively, at some time during the preceding 10 days. Shown are the mean fractions of air in the tropospheric column having such influences. Note that these conditions are not exclusive, as parcels experiencing rapid vertical motion may encounter both the boundary layer and stratosphere within a 10-day history. Lagrangian mean stratospheric influence is largest at latitudes between 20 and 50 N with peak values of about 30%. The pattern of largest stratospheric influence broadly follows the location of the summertime subtropical jet stream, although a maxima also occurs in the vicinity of the Bermuda High, associated with the persistent large-scale descent in this region. Largest PBL influence, in excess of 60%, is generally associated with tropical convection. Significant PBL influence also occurs over the midlatitude continents and extends eastward over the oceans. This pattern is consistent with daytime boundary layer growth and ventilation over the continents combined with frontal lifting and eastward continental outflow [e.g., Cooper et al., 2002]. PBL influence is low in midlatitude oceanic regions dominated by large-scale descent (Bermuda high, Pacific high).

Figure 3 shows the Lagrangian mean net photochemical production of O3 segregated by upper free troposphere (7 km to tropopause), lower free troposphere (edge of boundary layer to 7 km), and boundary layer. Positive values indicate net production and negative values indicate net destruction. In the boundary layer net production dominates over most continental regions. Net destruction is found over all oceanic regions and over most subtropical continental regions. Largest magnitudes of net production, approximately 13 ppbv/day, are more than double the

largest magnitudes of net destruction. In the lower free troposphere the balance shifts more toward net destruction although production still exists over much of midlatitude North America and Eurasia. The largest magnitudes of net destruction are associated with the strong convection in the Gulf/Caribbean and East Asia (c.f. Figure 2). In the upper free troposphere net production is found everywhere except for regions experiencing convective influence. In summary, Lagrangian mean net destruction of O3 is found at all altitudes in regions experiencing strong convection. That this occurs is explained by considering that O3 concentration generally increases from the surface to the tropopause and that strongest destruction generally occurs in the clean maritime lower troposphere. Air moving from the O3-rich upper troposphere to the maritime boundary layer experiences rapid O3 destruction after descent. At higher altitudes in these convective regions the signature of net destruction reflects large-scale Lagrangian ascent (not shown).

In addition to transport and photochemical production the O3 budget in the RAQMS model is influenced by the assimilation of satellite O3 observations [Pierce et al., this issue]. The bottom panel of Figure 3 shows the effect of assimilation on O3 in the boundary layer. Shown is the PBL-averaged Lagrangian mean O3 increment resulting from the assimilation of column O3 data. Largest changes are positive and negative 0.7 ppbv, or about 2% of the PBL-averaged O3 mixing ratio. The sign of the assimilation increment is generally opposite to the net photochemical tendency (panel (c)) and largest changes occur where the photochemical tendency is largest, suggesting an imbalance between the photochemical prediction and assimilation. This suggests that either the model overestimates both strong production and destruction or the satellite measurements (in this case cloud cleared TOMS total column O3) do not capture the true PBL ozone variability. The TOMS V8 retrieval algorithm captures only 50% of the variance

below 5 km [TOMS Version 8 Algorithm Theoretical Basis Document, available at http://toms.gsfc.nasa.gov/version8/v8toms_atbd.pdf]. In the current RAQMS approach to column ozone assimilation we account for the altitude dependence of the TOMS sensitivity and remove the influence of the TOMS apriori in constructing the first guess but the resulting column assimilation increment is distributed uniformly (by mass) throughout the column. We may find a smaller imbalance between photochemistry and assimilation if we incorporate the altitude dependence of the TOMS sensitivity in the redistribution of the column assimilation increment through the column, thereby applying less mass adjustment where TOMS is less sensitive. Assimilation increments averaged over the lower and upper troposphere are similar to the distribution shown here but smaller in magnitude. We conclude that the mean influence of assimilation is at most on the order of 10% of the photochemical O3 budgets analyzed here.

Figure 4 shows maps of Lagrangian mean NOx and PAN concentrations averaged over the lower free troposphere and the boundary layer. Parcels experience very large Lagrangian mean NOx concentrations at the surface near primary source locations: Western Europe, Northeastern US, and Northern China. Peak Lagrangian mean mixing ratios of almost 2 ppbv are found locally in Europe. Lower tropospheric Lagrangian mean NOx also shows that air parcels experience high concentrations in these industrialized regions but additionally shows largest influences emanating from Alaska and Western Canada. This peak is due to the extensive biomass burning that occurred during July 2004 [Pfister et al., 2005, this issue; Soja et al., this issue] and is associated with enhanced O3 production (Figure 3). Overall it can be seen that Lagrangian mean photochemical production of O3 in the troposphere is correlated with exposure to NOx as expected. However NOx is relatively short-lived in the lower troposphere and concentrations drop rapidly away from primary source regions, particularly near the surface. PAN is of interest

to the O3 budget in the context of long-range transport because it is relatively long-lived in the mid to upper troposphere but thermally decomposes to release NOx in the lower troposphere. Formed from NO2 and hydrocarbon oxidation products, Lagrangian mean PAN exposure has a similar distribution to Lagrangian mean NOx exposure in the boundary layer but much smaller concentrations – about a factor of 5 smaller. In the lower free troposphere PAN and NOx have similar concentrations but PAN is additionally found at locations far removed from NOx emissions. In fact, Lagrangian mean PAN exposure is nearly ubiquitous in the midlatitude lower free troposphere, having a relative minimum over the Pacific. A broad pool of high PAN exposure is evident over Eastern Canada and the Northeastern U.S. to the southeast of a tongue of even higher PAN exposure emanating from Alaska and Yukon. This feature is again a signature of the summer 2004 wildfires. The Lagrangian mean shows that air exposed to high PAN concentrations resulting from NOx and hydrocarbon precursors emitted by burning is then advected to the southeast and entrained into the low pressure region prevailing over Eastern Canada during July 2004 [e.g., Fuelberg et al., this issue].

CONUS Analysis: Zonal Cross Sections and Source/Receptor Categories

Shown in Figure 5 are zonally averaged cross sections over CONUS (longitudes between 125W and 65W) of the 10-day Lagrangian averaged quantities used in forming the airmass selection criteria. The mean thermal tropopause and the latitudes of the southern and northern boundaries of the CONUS domain are shown for reference in each panel. The motivation for the subsequent selection criteria is to identify the dominant properties controlling the chemical distribution of air within CONUS, including long-range transport and interactions with convectively and stratospherically influenced air, factors contributing to airmass chemical transformation including local sources and the marine boundary layer, and the influence of

specific sources including Asia and the Alaskan wildfires. Thus the particular quantities shown in Figure 5 are those expected to have a strong influence on either the transport or photochemical evolution of O3.

Strongest Lagrangian mean O3 photochemical tendencies over CONUS are negative, with peak values in excess of -4 ppbv/day, in the southern lower troposphere. Lagrangian mean O3 photochemical tendencies are positive in the upper troposphere and northern lower troposphere, maximizing near the surface and tropopause at about 2 ppbv/day. Lagrangian averaged O3 convective mixing tendencies are positive in the lower troposphere, maximizing in the south and near the surface, and negative in the upper troposphere. Over CONUS the Lagrangian mean convective and photochemical tendencies have similar magnitudes and, except for the northern lower troposphere, opposing signs. Lagrangian mean PAN exposure is seen to be pervasive throughout the troposphere over CONUS except for the southernmost lower troposphere. Lower troposphere enhancements in PAN exposure to the north of CONUS, as noted above, are associated with biomass burning and are correlated with enhanced Lagrangian mean photochemical production of O3 (panel a). Lagrangian mean stratospheric influence is generally aligned with the mean tropopause location, maximizing just below the tropopause at 60-70%. There are two distinct maxima separated by the midlatitude tropopause break at about 45N. Lagrangian mean stratospheric influence extends down to 8-10 km over northern CONUS but only to 13 km over southern CONUS. Mean Lagrangian large-scale mixing exposure maximizes in the upper troposphere near 45N, associated with the mean location of the midlatitude jet, and is also strong in the CONUS lower troposphere. Lagrangian mean mixing is relatively weaker in the southernmost CONUS upper troposphere. Finally, Lagrangian mean NOx exposure due to lightning peaks at about 90 pptv/day in the mid-upper troposphere near 30N. Lagrangian mean

NOx mixing ratios (not shown) are about 100 pptv at 10 km over CONUS, suggesting that lightning is a significant source of upper tropospheric NOx in summer.

The cross sections shown in Figure 5 together with the maps shown in Figure 2-Figure 4 provide the context needed for defining airmass categories for the CONUS receptor region. To reiterate, the next phase of the analysis is the selection of parcels that are located within the CONUS domain at the end of a 10-day period and that have specific combinations of geospatial and/or 10-day Lagrangian averaged chemical and dynamical characteristics. These categories are summarized in Table 1 and the associated criteria are labeled with white numerals corresponding to the category number in the panels of Figure 5 (where possible).

Category 1 focuses on the influence of long-range pollution transport coupled with convective mixing, illustrated by characteristics evident in the upper northern quadrant of the CONUS domain in Figure 5, and includes parcels arriving in the CONUS upper troposphere (altitude greater than 7km) that have experienced strong Lagrangian mixing, negative O3 convective tendency, and mean O3 net photochemical production of at least 0.1 ppbv/day. Category 2 focuses on long-range pollution transport with stratospheric influence and is also guided by the upper northern quadrant; characteristics are arrival in the upper troposphere, stratospheric influence, strong mixing, and O3 production greater than 0.1 ppbv/day. Category 3 focuses on airmass chemical transformation and, guided by the lower northern quadrant, considers parcels in the lower troposphere that have experienced O3 production. Category 4 focuses on maritime influence, guided by the lower southern quadrant, and considers lower tropospheric air that has experienced strong net destruction of O3 (at least -2.0 ppbv/day) and a positive O3 convective tendency. Category 5 specifically focuses on East Asian influence and considers parcels that have either been within the East Asian boundary layer or have experienced

convection while over East Asia. Category 6 focuses on O3 production associated with lightning NOx, considering parcels experiencing O3 production and a lightning NOx source of at least 50 pptv/day. Category 7 focuses on the pervasive PAN reservoir in the mid-troposphere and associated O3 production (mean PAN concentrations of at least 175 pptv and O3 production greater than 0.1 ppbv/day). Category 8 focuses specifically on influences of the Alaska/Yukon fires evident in large lower tropospheric PAN values to the north of CONUS with collocated O3 production (PAN > 500 pptv, O3 production > 0.1 ppbv/day).

CONUS Analysis: Airmass Origins

The geospatial origin, or location 10 days prior, of air influencing the CONUS receptor region and exhibiting the characteristics of these eight categories is analyzed by considering probability density functions (PDFs) with respect to longitude, latitude and altitude (Figure 6). These distributions of airmass origin are determined within bins of 10 degrees in latitude and longitude and 1 km in altitude. For conciseness the distributions are presented as sets of two-dimensional PDFs created by summing in the third dimension: latitude-longitude column sums, altitude-longitude meridional sums, and altitude-latitude zonal sums. Because the PDFs are normalized distributions, the fraction of parcels satisfying the selection criteria is also noted on the figure to provide a measure of the relative frequency of occurrence of air exhibiting these properties. We focus primarily on Lagrangian characteristics over 10-day back trajectories but the interpretation is aided by also considering shorter periods (not shown) and the selection fractions are summarized in Table 1 for back trajectory times of 1, 4, and 7 days in addition to 10 days.

Category 1: Transport and Convective Mixing with O3 Production

Air defined by Category 1 has signatures of both long-range and regional transport. Airmasses originate primarily in and around the Gulf of Mexico with additional source locations along a band extending westward across the Pacific into central Asia. Air satisfying these criteria comprises about 15% of all CONUS air above 7 km and the principal arrival location is over the southwestern part of the domain at about 9 km. Note that the fraction of parcels satisfying these criteria remains nearly constant within back trajectory periods of 1-10 days, suggesting that at least some of these conditions (probably convection) were experienced within a day of arrival. The Gulf origin is largest below an altitude of 5 km but extends upward and westward to about 10 km. Air originating below 7 km has experienced large-scale ascent in order to arrive above 7 km. The air from the Pacific and Asia originates at higher altitudes, nominally about 10 km. Airmasses from these two distinct source regions come together over the southwestern US in the mid-troposphere where they likely experience convection (note the local convection maxima in Figure 1(d)) which results in the negative O3 convective tendency (mixing ratio decreased by convective exchange).

Category 2: Transport and Stratospheric Influence with O3 Production

Parcels defined by Category 2 characterize 16.4% of all CONUS air above 7 km. Source locations at 10 days back extend across the Pacific and into central Asia, as observed with Category 1, but are consistently at high altitude. In the vertical these parcels originate in a layer just above the high-altitude parcels defined by Category 1, aligned with the mean tropopause (Figure 5). The western Pacific is the predominant source location at 10 days back but there is also a Gulf of Mexico component. The fraction of parcels satisfying these criteria declines by about half between 4 days back, when most parcels are still over the central Pacific, and 1 day

back when most parcels are over the northwestern US. This behavior is consistent with the analysis of Postel and Hitchman [1999] who show the central Pacific to be a preferred region for stratosphere/troposphere exchange during this time of year. Overall this category reflects a dominant influence of long-range transport from the Pacific and Asia combined with a smaller regional influence from subsidence associated with pervasive high pressure in the eastern Gulf of Mexico.

Category 3: Airmass Chemical Transformation

Category 3 defines about half of the CONUS air below 7 km. The 10-day airmass origin shows two distinct peaks, one over south central Canada and one over the Gulf of Alaska, located almost entirely within the lowest 1 km of the atmosphere. Air with Canadian origin slowly moves south during the trajectory period to arrival over the upper Midwest while the maritime air follows the coastline to the US Pacific Northwest and then moves eastward to arrive over a broad region between the northern Rockies and upper Midwest. The fraction of parcels remains relatively constant between 10 and 1 days back indicating that O3 production is occurring within a day of arrival. This category provides a clear example of airmass transformation as relatively clean maritime air from the Gulf of Alaska moves over the northern US where it experiences O3 production (Figure 3) upon exposure to O3 precursors including NOx (Figure 4). The interpretation of the grouping from Canada is more ambiguous regarding the timing of O3 production as this source region shows appreciable NOx concentrations and O3 production in the lower free troposphere at 4-7 days back (associated with the wildfires), but significantly larger values of both NOx and O3 production within the boundary layer on moving south of the Great Lakes at 1-4 days back.

Category 4: Maritime Influence

Category 4 parcels originate mainly near the surface over a broad region centered over the Gulf of Mexico. Parcel origins also include a tongue extending eastward across much of the Atlantic around the southern periphery of the Bermuda High, and arrival location for this air is the southwestern CONUS lower troposphere. This airmass is primarily maritime air that has traveled westward around the Bermuda High and over the Gulf. The fraction of parcels increases with number of days back suggesting that fewer parcels exhibit these mean characteristics as the airmasses move over land. This trend is supported by the distributions shown in Figure 2 and Figure 3 where it is seen that convective mass flux and lower tropospheric Lagrangian-averaged O3 destruction are strongest over the Caribbean and Gulf. Persistent deep convection over the Gulf results in the positive O3 convective tendency. By comparison with source Category 1 this relatively clean maritime air is collocated with convectively entrained free tropospheric air, some of which has Pacific and Asian origin.

Category 5: Asian Influence with O3 Production

Category 5 defines only about 2% of all tropospheric air arriving over CONUS within 10 days. This fraction increases to 3% if the photochemical tendency is not considered (not shown). As expected the fraction of parcels decreases rapidly for back trajectory periods shorter than 10 days. Airmass origin is centered over eastern China at about 8 km showing that most of the influence results from exposure to convection over Asia rather than direct transport from the Asian boundary layer. These features are consistent with estimates of Holzer et al. [2005] who show that while trans-Pacific transport from Asia is largest in winter/spring, summer transport from East Asia to North America is primarily aloft with mean transit time of 6-8 days.

Category 6: Lightning NOx Influence with O3 Production

Category 6 describes 12.4% of all tropospheric air over CONUS. The western Gulf of Mexico is the predominant 10-day origin however air also arrives from Canada, the Pacific, and Central America. There are two distinct populations in the vertical: a surface layer, particularly north of 40N, and a broad mid-tropospheric region mainly south of 40N. The lightning NOx source is triggered by convection and has a C-shaped vertical profile [Pickering et al., 1998; Allen and Pickering, 2002]. The higher-altitude branch is of particular interest because lightning appears to be the dominant NOx source in the upper free troposphere (see discussion of Figure 5). The low altitude branch may be an important NOx source over non-urban and maritime areas but otherwise its influence on the O3 budget is difficult to distinguish against the background of generally high NOx from surface emissions. The fraction of parcels in this category is relatively constant between 1 and 10 days back and the primary arrival location (at 1 day back) is over the Plains states. Parcels arrive from the north mainly at low altitude and from the south mainly at high altitude, while parcels from the west arrive at both high and low altitude and remain a distinct secondary population. Together, these characteristics indicate convective detrainment of photochemically processed air over the Gulf and the Plains states and separate convective processing of western air over the desert southwest.

Category 7: PAN Reservoir with O3 Production

Category 7 is designed to characterize the PAN reservoir evident in the free troposphere, of interest because of its potential for conversion to NOx and subsequent O3 production. Airmass origin is primarily North America with a small contribution from East Asia. More than 20% of all tropospheric parcels are included in this category between 1 and 10 days back. The altitude/latitude PDF shows two distinct peaks among a very broad population. The largest

population extends over most of CONUS and is centered in the upper troposphere at 35N while the second population is centered at lower altitude (1.5 km) farther north. The high altitude population is a combination of air coming from Asia, the Pacific, and North America. Given the long lifetime of PAN in the upper troposphere this air is a mixture of well aged pollution that has experienced long range transport and fresher regional pollution from North America that ascends into the upper troposphere within a 10-day timescale. The low altitude population extends across most latitudes of North America but is centered at 55N. PAN thermally decomposes at these altitudes so concentrations result from equilibrium between decay and fresh regional production from NOx and hydrocarbon emissions.

Category 8: Alaska/Yukon Fires with O3 production

The final category focuses on characterizing the influence of the large wildfires burning in Alaska and Yukon. With these criteria the 10-day origins show a population coming from that region at an altitude of 2-6 km, yet a second population with origins near the surface in the Great Lakes region also exists. Parcels in this category describe 2.6% of all CONUS air below 7 km, of which we estimate that about 1% is a direct influence of the wildfires. (The total fraction of parcels in this category increases to over 7% at 1-day back, but the dominant origin is the boundary layer of the Ohio River valley.) Most of the outflow from these fires remains to the north of the CONUS domain, as evidenced by the large region of enhanced PAN over eastern Canada (Figure 4). As shown by the analysis of Category 7 a significant fraction of CONUS air with moderately enhanced PAN comes from central Canada within a 10-day period. Within a 10-day period, the air in central Canada having enhanced PAN comes primarily from the fires (source analysis using a southeastern Canada receptor region, not shown). Thus the influence of the fires on CONUS is likely somewhat larger than indicated here but occurs over longer time

scales of 10-20 days. Overall the influence of the fires on the mean CONUS O3 budget during the mission is small and comparable to the Asian influence.

CONUS Summary

Approximately half the air in the lower troposphere experiences O3 production within the domain on exposure to local emissions (Category 3). There is a striking collocation over the Gulf and southern CONUS of air experiencing strongest O3 destruction in the lower troposphere (Category 4) with upper tropospheric air experiencing convection and O3 production (Category 1). This couplet shows the influence of deep convection as relatively O3-rich air from the upper troposphere is convectively mixed down to the maritime lower troposphere, where it experiences rapid destruction, and lower tropospheric air rich with fresh emissions is convectively mixed to the upper troposphere, where it experiences O3 production. Air experiencing O3 production associated with exposure to lightning NOx (Category 6) also originates primarily over the Gulf and southern CONUS. The persistence of this summer convective influence has previously been noted by Li et al. [2005] who find that O3 production occurs within the semipermanent upper tropospheric anticyclone over the southern U.S. following convective lofting of precursors and the additional influence of lightning NOx. Also consistent with this influence, approximately half of the air in the CONUS free troposphere associated with enhanced PAN (Category 7) originates in the mid-troposphere over the Gulf. We find that approximately 16% of CONUS air above 7 km is stratospherically influenced and experiences O3 production, originating primarily in the central Pacific and Asia. Thompson et al. [this issue] estimate a mean stratospheric component of 26% by O3 mass content in the upper troposphere over an area corresponding to the northeast of our CONUS domain. The differences in these estimates may arise from comparison of different domains, however removing our condition on O3 production and expressing our frequency-based

estimate in terms of O3 mass would both increase our fraction, moving these estimates into better agreement. In the mean we find that Asian emissions and the Alaska/Yukon fires have very little direct influence on CONUS O3 within a 10-day exposure.

Liang et al. [this issue] use a principal component analysis to estimate influences of different airmass categories on air sampled by the DC-8 during INTEX-A. To better compare results of these different techniques we have assessed airmass fractions associated with Asian, stratospheric, and convective influences within the altitude range 6-12 km. No other selection criteria, such as conditions on O3 production, are applied. Our resulting estimates are 9% East Asian influence, 12% stratospheric influence, and 12% convective influence (using a Lagrangian mean convective threshold of 75 mbar/day to define strong convection). Liang et al. [this issue] find fractions of 7% Asian, 6% stratospheric, and 13% strong convection. The agreement is quite good for the Asian and convective influences, suggesting that the sampling pattern of the DC-8 during INTEX-A was representative of the mean CONUS exposure for these airmass types. That our estimate of stratospheric influence is larger than the DC-8 based estimate by Liang et al. [this issue] may suggest that stratospherically-influenced air was statistically under-sampled by the DC-8.

Europe Analysis: Zonal Cross Sections and Source/Receptor Categories

Figure 7 shows 10-day Lagrangian mean quantities zonally averaged over the range of longitudes of the European domain (15W-30E) during July 11-August 15, 2004. Locations of the mean thermal tropopause and southern and northern boundaries of the domain are shown in each panel. To first order the patterns are similar to those seen in the CONUS cross sections but there are important differences. The Europe domain is farther north than the CONUS domain and as a result is characterized by a lower mean tropopause height. The Lagrangian mean net

photochemical destruction of O3 in the lower troposphere is weaker over Europe and does not extend down to the surface as it does over the southern portion of the CONUS domain. The Lagrangian mean O3 convective tendencies are also smaller over Europe. These relative characteristics likely reflect weaker convection and maritime coupling associated with the Mediterranean compared with the strong maritime and convective influences of the Gulf of Mexico over southern CONUS (e.g., Figure 2(a), Figure 3(c)). Lagrangian mean net photochemical production of O3 at the surface is stronger over Europe. The mid-tropospheric maximum in Lagrangian mean PAN exposure is larger over Europe, however the lower tropospheric peak seen on the northern boundary of CONUS (and collocated enhancement in O3 production) associated with the wildfires is absent over Europe. Peak values of Lagrangian mean stratospheric influence are similar at about 70% but stratospheric influence extends over a larger fraction of the European domain in the vertical because of the lower mean tropopause height at these higher latitudes. The tropopause break, collocated with the minimum in stratospheric influence, and the associated peak in Lagrangian mean mixing efficiency are at the southern edge of the European domain but near the northern edge of the CONUS domain. Peak mixing efficiency is also stronger over Europe. Finally, the Lagrangian mean lightning NOx exposure is smaller over Europe than CONUS but much larger exposure values are found in latitudes to the south of the Europe domain.

As noted above we have used similar sets of selection criteria for the CONUS and Europe airmass categories. The main differences are that for Europe we consider a CONUS influence region (Category 5) instead of an Asian influence, and within Category 4 a convective criterion is less compelling than for CONUS (because values are significantly smaller) so is omitted. Also, because of the diminished vertical domain resulting from the lower tropopause, 6 km instead of 7

km is used as the boundary between upper and lower troposphere. The selection criteria categories are labeled on the relevant characteristics in Figure 7 and summarized in Table 2.

Europe Analysis: Airmass Origins

Probability density functions showing 10-day airmass origins for each of the 8 selection categories of the Europe receptor region are shown in Figure 8. Percentages of parcels satisfying the criteria at different back trajectory periods are given in Table 2. Primary attention is focused on differences in behavior relative to the CONUS discussion.

Category 1: Transport and Convective Mixing with O3 Production

The primary source region for Category 1 is the midlatitude upper troposphere of the eastern Pacific and North America, centered on the US west coast. At 10 days back the fraction of upper tropospheric parcels included in this category is 15.5%, very similar to CONUS Category 1, but for Europe there is almost no local source component whereas CONUS has a large local/regional component. The percentage of parcels included in this category decreases with shorter back trajectory periods (in contrast to CONUS) but is still over 7% at 1-day back at which time these parcels are over the northern Mediterranean, evidently the only location within Europe where strong mixing and negative O3 convective tendency are coincident. Overall these parcels have experienced long-range transport over a 10-day period, almost half experience the characteristics of this category over the Mediterranean during the previous day, and the rest experience the characteristics over North America and the eastern Pacific.

Category 2: Transport and Stratospheric Influence with O3 Production

Airmass origins for Category 2 have characteristics similar to those for CONUS: origins are in the upper troposphere well to the west of the receptor domain. The principal origin is the Pacific, primarily eastern, and a secondary peak is found in the southwestern Atlantic associated

with the Bermuda High. These origin locations are coincident with regions of enhanced stratospheric influence to the west of Europe as shown in Figure 2(b). At 10-days back the fraction of parcels is 21%, about 5% larger than found for CONUS. The fraction at 1-day back is about half that at 10-days back, a similar trend as found for CONUS. Parcel origins for this category are generally collocated with those of Category 1 but at higher altitudes.

Category 3: Airmass Chemical Transformation

The parcel characteristics for Category 3 are also similar to those of the CONUS receptor region. More than half the lower tropospheric parcels are included in this category and the primary region of origin is relatively clean, in this case the low altitude North Atlantic. The fraction of parcels is relatively constant from 1 to 10 days back, suggesting that production occurs within a day of arrival. At 1-day back most of the parcels are located within the receptor region. Regional photochemical transformation occurs as the parcels encounter fresh emissions within the domain.

Category 4: Maritime Influence

Category 4 focuses on strong O3 destruction in the lower troposphere. A criterion on O3 convective tendency, included in this category for the CONUS receptor, is omitted because convective tendencies are much smaller over Europe; inclusion of the convection criterion (not shown) results in a similar distribution of airmass origins as shown here but a much smaller number of parcels (factor of 3.5 smaller). The dominant 10-day origin of these parcels is the western Atlantic lowermost troposphere and a secondary cluster of origins is found over northwest Africa. The fraction of parcels is relatively constant from 10-days to 1-day back, increasing by only 2%. At shorter periods back parcels also tend to be located in maritime environments including the Mediterranean (the focus of parcels arriving from Africa) and the

North Sea. These features indicate that air influencing Europe that has experienced strong net O3 destruction has likely had significant maritime influence.

Category 5: CONUS influence with O3 production

Category 5 includes 9.4% of all parcels arriving in the Europe domain. The 10-day origins include most of CONUS and also extend beyond the CONUS boundaries, particularly to the west. The westernmost parcels originate at high altitude, suggesting they experience strong convective influence over CONUS rather than directly encounter the CONUS boundary layer. Origins of the eastern parcels are closer to the surface, centered at latitude 45N and longitudes between 90W and 60W, so these parcels likely have directly encountered the CONUS boundary layer and have subsequently experienced frontal lifting followed by long-range transport. This pathway is evident in the region of significant PBL influence over the north Atlantic, Figure 2(c). CONUS influence also includes 5.8% of all parcels at 7 days back and 1.4% at 4 days, indicating a population of parcels that experience rapid transport across the Atlantic in summer. Parcel origins at these ages are primarily high altitude.

Category 6: Lightning NOx Influence with O3 Production

Category 6 characterizes much less of the air over Europe than over CONUS, 3% versus 12%. Origins at 10-days back include a broad region of the free troposphere over CONUS and a distinct low-altitude region centered on southern Europe, probably associated with the Mediterranean. At shorter periods back this local area is the dominant origin, primarily near the surface, and the fraction of parcels remains near 3%.

Category 7: PAN Reservoir with O3 Production

Mean PAN concentrations in the mid troposphere are larger over Europe than CONUS and Category 7 characterizes about a quarter of all air over Europe (26%). In contrast to CONUS, the

largest population originates well outside the domain, coming from higher altitudes over North America and the Pacific. The air over the Pacific represents the well-aged PAN reservoir (i.e., the PAN was likely produced longer than 10 days ago) while the air over North America is a combination of aged (the higher altitudes) and fresher (lower altitudes) PAN production. Similar to the CONUS results, there is also a significant local/regional population at low altitudes. With these selection criteria it is not possible to determine whether these parcels are the result of recent local production of PAN and coincident O3 production from fresh NOx emissions, or decomposition of existing PAN leading to O3 production. Henne et al. [2005] identify a characteristic summertime phenomenon whereby mountain venting from the Alps influences the Mediterranean region as O3 production follows the release of NOx from PAN.

Category 8: Alaska/Yukon Fires with O3 production

Category 8 characterizes only about 1% of the Europe parcels but is noteworthy because it demonstrates that the influence of the Alaska/Yukon wildfires extends to Europe. The largest fraction of this population is located between 3 and 6 km over the location of the fires. There is also a smaller local population at the surface, so the mean influence of the fires on Europe is somewhat less than 1%.

Europe Summary

Similar to CONUS, over half the air in the lower troposphere experiences O3 production within the domain upon exposure to local emissions following transport from relatively clean source regions (Category 3). Strong O3 destruction in the lower troposphere (Category 4) is associated with maritime exposure. Approximately 21% of upper tropospheric air is associated with stratospheric influence and O3 production (Category 2), about a 5% larger fraction than found over CONUS. Upper tropospheric air with stratospheric and strong mixing influences has

its primary origin in the eastern Pacific, consistent with Penkett et al. [2004] who find evidence for long-range transport of pollution from the west coast of the U.S. interspersed with stratospherically influenced air. About 9% of all tropospheric air has experienced O3 production associated with direct CONUS influence (Category 5). The influences of convection and lightning NOx are smaller than found over CONUS. The mid-tropospheric PAN reservoir (Category 7) describes about a quarter of all free tropospheric air and has large contributions from both remote and local source regions.

Other investigators have found similar evidence for this summer influence of North America on European O3. Auvray and Bey [2005] find that North American O3 fluxes into Europe maximize in spring and summer due to enhanced photochemical activity and relatively direct transport pathways associated with deep convection over North America and zonal flow over the North Atlantic. Auvray and Bey [2005] conclude that North America contributes about 10% to the O3 budget of Europe in summer, in good agreement with our estimate of 9%. Trickl et al. [2003] identify different long-range transport pathways contributing to summer ozone events in Europe. While they find evidence for direct export from the North American boundary layer, including contributions from large-scale convection and frontal advection, they also note entrainments from source areas beyond North America associated with stratospheric and Asian influence.

Conclusion

We have applied a novel technique in which source/receptor relationships are established through Lagrangian sampling of Eulerian dynamical/chemical fields and cluster analysis of resulting distinct features. Using this technique we have characterized the dominant contributions to the O3 distributions over the continental U.S. and Europe. Where possible we have compared

our results with other approaches to verify our technique. Our main findings are summarized here.

Within the lower troposphere of both CONUS and Europe about half the air experiences O3 production associated with exposure to local precursor emissions. In both regions this air tends to come from relatively clean source regions: the Pacific and Canada for CONUS, and the North Atlantic for Europe. Within the lower troposphere of both regions, about 13% of air experiences strong O3 destruction associated with exposure to the maritime boundary layer. Over CONUS this air is also associated with strong convective mixing over the Gulf of Mexico. Stratospheric and mixing influence associated with O3 production in the upper troposphere characterizes 16 and 21% of the air over CONUS and Europe respectively. For both CONUS and Europe the primary source region is well to the west, over the Pacific, a preferred zone for stratosphere/troposphere exchange in summer [Postel and Hitchman, 1999]. Enhanced PAN in the mid-troposphere associated with O3 production characterizes both CONUS and Europe, however for CONUS the source of this air is primarily regional while for Europe there is a significant long-range contribution from North America. The large wildfires in Alaska and Yukon have very little direct influence (less than 1%) on the air in either CONUS or Europe within a 10-day exposure but may have a larger influence if periods longer than 10 days are considered.

The largest differences between CONUS and Europe are associated with persistent deep convection in the Gulf of Mexico and southern U.S. Exposure to lightning NOx (triggered by convection) with associated O3 production characterizes 12% of all tropospheric air over CONUS but only 3% over Europe. For CONUS, the Gulf convection is a center of action in which influences from long-range transport, local precursor emissions (anthropogenic and

lightning), and regional photochemistry are linked. While there is no such strong unifier for air influencing Europe, we find evidence that the convection over the U.S. contributes to the long-range transport from the U.S. to Europe in summer.

Within the contexts of INTEX and ICARTT we find relatively little direct Asian influence on ozone over the U.S. during the summer of 2004 (2%) but a sizeable U.S. influence on Europe (9%). These estimates are consistent with other estimates in the literature for summer ozone. We have additionally identified a strong convective coupling between long-range pollution transport and ozone in the U.S. boundary layer. Implementation of abatement strategies for ground level ozone associated with LRTAP must consider the interplay between anthropogenic and natural components inherent in the processes contributing to these transboundary pollution transports.

References

Allen, D. J., and K. E. Pickering, Evaluation of lightning flash rate parameterizations for use in a global chemical transport model, J. Geophys. Res., 107(D23), 4711, doi:10.1029/2002JD002066, 2002.

Auvray, M., and I. Bey, Long-range transport to Europe: Seasonal variations and implications for the European ozone budget, J. Geophys. Res., 110, D11303, doi:10.1029/2004JD005503, 2005.

Cooper, O. R., J. L. Moody, D. D. Parrish, M. Trainer, T. B. Ryerson, J. S. Holloway, G. Hubler, and F. C. Fehsenfeld, and M. J. Evans, Trace gas composition of midlatitude cyclones over the western North Atlantic Ocean: A conceptual model, J. Geophys. Res., 107(D7), 4056, 10.1029/2001JD000901, 2002.

Fairlie, T. D., R. B. Pierce, J. A. Al-Saadi, W. L. Grose, J. M. Russell III, M. H. Proffitt, and C. R. Webster, The contribution of mixing in Lagrangian photochemical predictions of polar ozone loss over the Arctic in summer 1997, J. Geophys. Res., 104(D21), 26,597–26,610, 1999.

Fast, J. D., Rahul A. Zaveri, Xindi Bian, Elaine G. Chapman, and Richard C. Easter, Effect of regional-scale transport on oxidants in the vicinity of Philadelphia during the 1999 NE-OPS field campaign, J. Geophys. Res., 107(D16), 4307, 10.1029/2001JD000980, 2002.

Fiore, A. M., Daniel J. Jacob, Isabelle Bey, Robert M. Yantosca, Brendan D. Field, Andrew C. Fusco, and James G. Wilkinson, Background ozone over the United States in summer: Origin, trend, and contribution to pollution episodes, J. Geophys. Res., 107(D15), 4275, 10.1029/2001JD000982, 2002.

Fuelberg, H. E., M. Porter, C.M. Kiley, D. Morse, A meteorological overview of the INTEX-A Period, this issue.

Henne, S., J. Dommen, B. Neininger, S. Reimann, J. Staehelin, and A. S. H. Prevot, Influence of mountain venting in the Alps on the ozone chemistry of the lower free troposphere and the European pollution export, J. Geophys. Res., 110, D22307, doi:10.1029/2005JD005936, 2005.

Holzer, M., T. M. Hall, and R. B. Stull, Seasonality and weather-driven variability of transpacific transport, J. Geophys. Res., 110, D23103, doi:10.1029/2005JD006261, 2005.

Li, Q., D. J. Jacob, I. Bey, P. I. Palmer, B. N. Duncan, B. D. Field, R. V. Martin, A. M. Fiore, R. M. Yantosca, D. D. Parrish, P. G. Simmonds, and S. J. Oltmans, Transatlantic transport of pollution and its effects on surface ozone in Europe and North America, J. Geophys. Res., 107(D13), 4166, 10.1029/2001JD001422, 2002.

Li, Q., D. J. Jacob, J. W. Munger, R. M. Yantosca, and D. D. Parrish, Export of NOy from the North American boundary layer: Reconciling aircraft observations and global model budgets, J. Geophys. Res., 109, D02313, doi:10.1029/2003JD004086, 2004.

Li, Q., D. J. Jacob, R. Park, Y. Wang, C. L. Heald, R. Hudman, R. M. Yantosca, R. V. Martin, and M. Evans, North American pollution outflow and the trapping of convectively lifted pollution by upper-level anticyclone, J. Geophys. Res., 110, D10301, doi:10.1029/2004JD005039, 2005.

Liang, Q., L. Jaeglé, R. Hudman, S. Turquety, D. Jacob, M. Avery. G. Sachse, D. Blake, E. Browell, W. Brune, X. Ren, R. Cohen, J. Dibb, G. Huey, H. B. Singh, P. Wennberg, L. Pfister, H. Fuelberg, Summertime influence of Asian pollution in the middle and upper troposphere during INTEX-A, this issue.

Penkett, S. A. et al., Long-range transport of ozone and related pollutants over the North Atlantic in spring and summer, Atmos. Chem. Phys. Discuss., 4, 4407–4454, 2004.

Pfister, G., G. Pétron, L. K. Emmons, J. C. Gille, D. P. Edwards, J.-F. Lamarque, J.-L. Attie, C. Granier, and P. C. Novelli, Evaluation of CO simulations and the analysis of the CO budget for Europe, J. Geophys. Res., 109, D19304, doi:10.1029/2004JD004691, 2004.

Pfister, G., P. G. Hess, L. K. Emmons, J.-F. Lamarque, C. Wiedinmyer, D. P. Edwards, G. Petron, J. C. Gille, and G. W. Sachse, Quantifying CO emissions from the 2004 Alaskan wildfires using MOPITT CO data, Geophys. Res. Lett., 32, L11809, doi:10.1029/2005GL022995, 2005.

Pfister, G. et al., Ozone Production from Boreal Forest Fire Emissions, this issue.

Pickering, K. E., Y. Wang, W. K. Tao, C. Price, and J. F. Muller, Vertical distributions of lightning NOx for use in regional and global chemical transport models, J. Geophys. Res., 103, D23, 31,203-31,216, 1998.

Pierce, R. B., J. Al-Saadi, C. Kittaka, D. Fairlie, T. K. Schaack, D. R. Johnson, T. H. Zapotocny, M. Avery, A. Thompson, R. Cohen, J. Dibb, J. Crawford, D. Rault, Jim Szykman, Randall Martin, Chemical data assimilation based estimates of Continental US Ozone and Nitrogen budgets during INTEX-A, this issue.

Postel, Gregory A. and Matthew H. Hitchman, A Climatology of Rossby Wave Breaking along the Subtropical Tropopause, J. Atmos. Sci., 56(3), 359–373, 1999.

Singh, H. B., W. Brune, J. Crawford, and D. Jacob, Overview of the Summer 2004 Intercontinental Chemical Transport Experiment-North America (INTEX-A), this issue.

Soja, A. J., J. A. Al-Saadi, R. B. Pierce, E. Alvaredo, C. Kittaka, W. McMillan, G. Sachse and J. J. Szykman, Description of a ground-based methodology for estimating boreal fire emissions for use in regional- and global-scale transport models, this issue.

Stohl, A., S. Eckhardt, C. Forster, P. James, and N. Spichtinger, On the pathways and timescales of intercontinental air pollution transport, J. Geophys. Res., 107(D23), 4684, doi:10.1029/2001JD001396, 2002.

Stohl, A., C. Forster, S. Eckhardt, N. Spichtinger, H. Huntrieser, J. Heland, H. Schlager, S. Wilhelm, F. Arnold, and O. Cooper, A backward modeling study of intercontinental pollution transport using aircraft measurements, J. Geophys. Res., 108(D12), 4370, doi:10.1029/2002JD002862, 2003.

Sutton, R. T., H. Maclean, R. Swinbank, A. O'Neill and F. W. Taylor, High-Resolution Stratospheric Tracer Fields Estimated from Satellite Observations Using Lagrangian Trajectory Calculations, J. Atmos. Sci., 51(20), 2995–3005, 1994.

Tao, Z., S. M. Larson, D. J. Wuebbles, A. Williams, and M. Caughey, A summer simulation of biogenic contributions to ground-level ozone over the continental United States, J. Geophys. Res., 108(D14), 4404, doi:10.1029/2002JD002945, 2003.

Thompson, A. M. et al., IONS-04 (INTEX Ozonesonde Network Study, 2004): Perspective on Summertime UT/LS (Upper Troposphere/Lower Stratosphere) Ozone over Northeastern North America, this issue.

Trickl, T., O. R. Cooper, H. Eisele, P. James, R. Mücke, and A. Stohl, Intercontinental transport and its influence on the ozone concentrations over central Europe: Three case studies, J. Geophys. Res., 108(D12), 8530, doi:10.1029/2002JD002735, 2003.

United Nations Economic Commission on Europe, Strategies and Policies for Air Pollution Abatement: 2002 Review prepared under The Convention on Long-range Transboundary Air Pollution, United Nations Publication E.03.11.E.49, 2004.

Weiss-Penzias, P., D. A. Jaffe, L. Jaegle, and Q. Liang, Influence of long-range-transported pollution on the annual and diurnal cycles of carbon monoxide and ozone at Cheeka Peak Observatory, J. Geophys. Res., 109, D23S14, doi:10.1029/2004JD004505, 2004.

Table 1. Definition of airmass selection criteria for each category in the CONUS receptor region and the percentages of parcels satisfying the criteria at 1, 4, 7 and 10 days back. FTU: Upper Free Troposphere. FTL: Lower Free Troposphere.

Category	Description	1-day	4-day	7-day	10-day
1	Strong Mixing, Negative O3 Convective Tendency, O3 Production, Z>7km	14.0% FTU	14.7% FTU	14.9% FTU	15.1% FTU
2	Stratspheric Influence, Strong Mixing, O3 Production, Z>7km	7.8% FTU	12.9% FTU	15.5% FTU	16.4% FTU
3	O3 Production, Z<7km	54.0% FTL	53.9% FTL	53.0% FTL	50.7% FTL
4	Strong O3 Destruction, Positive O3 Convective Tendency, Z<7km	9.7% FTL	11.7% FTL	13.0% FTL	13.6% FTL
5	Asian Influence, O3 Production	—	—	0.5% All	2.1% All
6	Lightning NOx > 50 pptv/day, O3 Production	14.1% All	14.7% All	13.6% All	12.4% All
7	PAN>175 pptv, O3 Production, Free Troposphere	23.4% All	22.6% All	21.7% All	20.5% All
8	PAN>500 pptv, O3 Production, Z<7km	7.2% FTL	5.2% FTL	3.3% FTL	2.6% FTL

Table 2. Definition of airmass selection criteria for each category in the Europe receptor region and the percentages of parcels satisfying the criteria at 1, 4, 7 and 10 days back. FTU: Upper Free Troposphere. FTL: Lower Free Troposphere.

Category	Description	1-day	4-day	7-day	10-day
1	Strong Mixing, Negative O3 Convective Tendency, O3 Production, Z>6km	7.3% FTU	10.7% FTU	14.1% FTU	15.5% FTU
2	Stratspheric Influence, Strong Mixing, O3 Production, Z>6km	9.9% FTU	16.4% FTU	19.7% FTU	21.1% FTU
3	O3 Production, Z<6km	55.9% FTL	54.2% FTL	53.8% FTL	54.9% FTL
4	Strong O3 Destruction, Z<6km	15.0% FTL	14.8% FTL	13.7% FTL	12.7% FTL
5	CONUS Influence, O3 Production	—	1.4% All	5.8% All	9.4% All
6	Lightning NOx > 50 pptv/day, O3 Production	2.9% All	2.3% All	2.5% All	3.0% All
7	PAN>175 pptv, O3 Production, Free Troposphere	28.9% All	27.4% All	26.6% All	26.0% All
8	PAN>500 pptv, O3 Production, Z<6km	4.0% FTL	2.2% FTL	1.2% FTL	0.9% FTL

Figure 1. Layer-averaged Eulerian mean quantities for period July 11-Aug 15 2004. (a) Boundary layer ozone. (b) Boundary layer ozone net production (line shows zero contour). (c) Upper troposphere (7km to tropopause) ozone. (d) Tropospheric mean convective mass flux.

Figure 2. 10-day Lagrangian mean during July 11-Aug 15 2004 of (a) tropospheric convective mass flux, (b) stratospheric influence, and (c) boundary layer influence.

Figure 3. 10-day Lagrangian mean ozone characteristics during July 11-Aug 15 2004. Net photochemical production averaged over (a) upper free troposphere (7km-tropopause), (b) lower free troposphere (PBL to 7km), and (c) PBL. (d) Mean O3 assimilation increment from column O3 constraint, averaged over PBL. Value of zero is contoured.

Figure 4. 10-day Lagrangian mean NOx and PAN during July 11-Aug 15 2004 averaged over the lower free tropopshere (PBL to 7km) and PBL. (a) FTL NOx. (b) PBL NOx. (c) FTL PAN. (d) PBL PAN.

Figure 5. 10-day Lagrangian mean zonal cross sections over CONUS domain during July 11-Aug 15 2004. (a) O3 net photochemical production. (b) O3 convective mixing tendency. (c) PAN concentration. (d) Stratospheric influence. (e) Mixing efficiency. (f) Lightning NOx source. Thick white lines show the mean thermal tropopause height and southern and northern boundaries of the domain.

Figure 6. PDF's of 10-day airmass origin for CONUS (Categories 1-4).

Figure 6. Continued (Categories 5-8).

1 Figure 7. 10-day Lagrangian mean zonal cross sections over Europe domain during July 11-Aug
2 15 2004. (a) O3 net photochemical production. (b) O3 convective mixing tendency. (c) PAN
3 concentration. (d) Stratospheric influence. (e) Mixing efficiency. (f) Lightning NOx source.
4 Thick white lines show the mean thermal tropopause height and southern and northern
5 boundaries of the domain.

6 Figure 8. PDF's of 10-day airmass origin for Europe (Categories 1-4).

7 Figure 8. Continued (Categories 5-8).

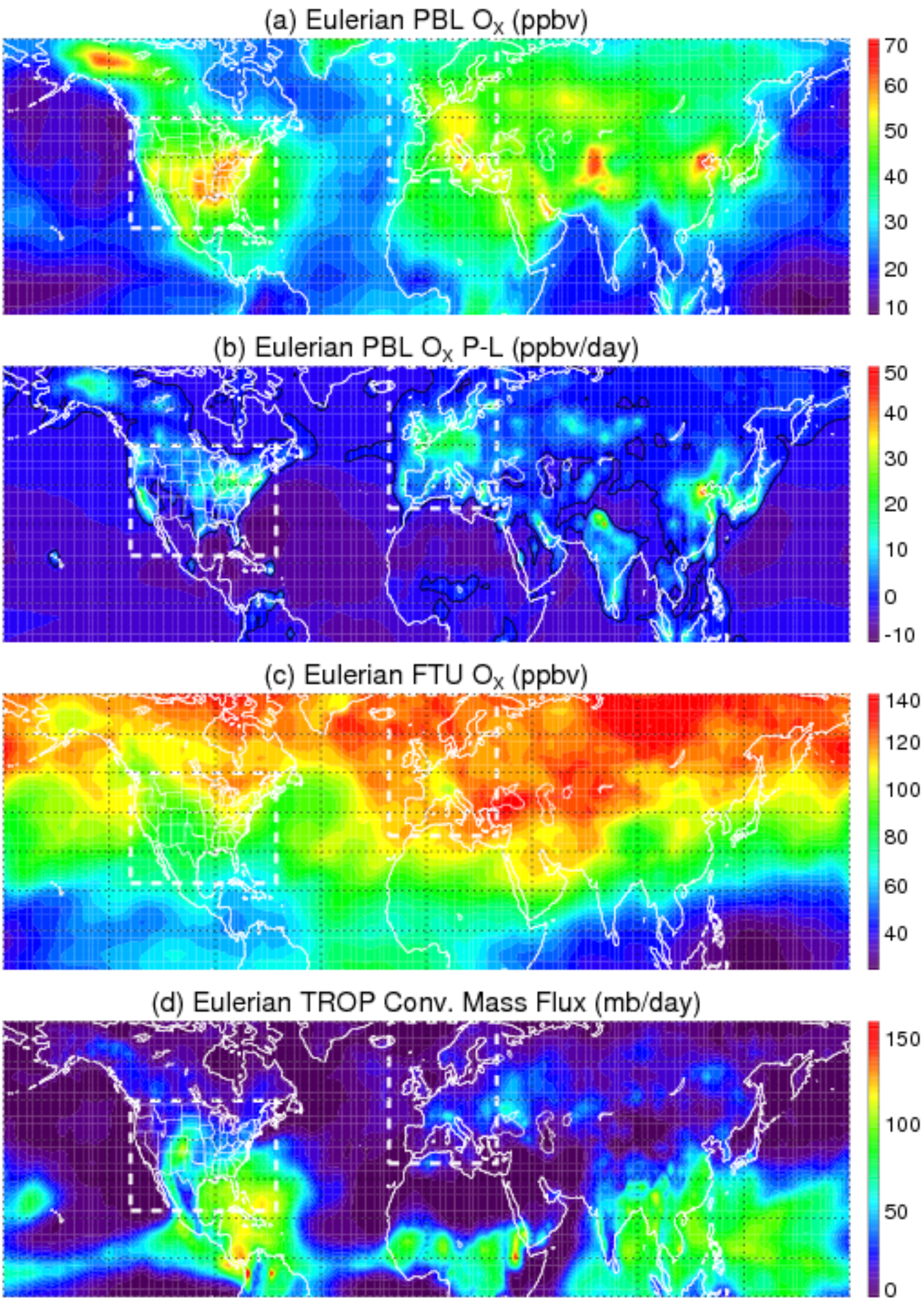
(a) Eulerian PBL O_X (ppbv)
70
60
50
40
30
20
10
(b) Eulerian PBL O_X P-L (ppbv/day)
50
40
30
20
10
0
-10
(c) Eulerian FTU O_X (ppbv)
140
120
100
80
60
40
(d) Eulerian TROP Conv. Mass Flux (mb/day)
150
100
50
0

(a) 10-day Lagrangian TROP Conv. Mass Flux (mb/day)

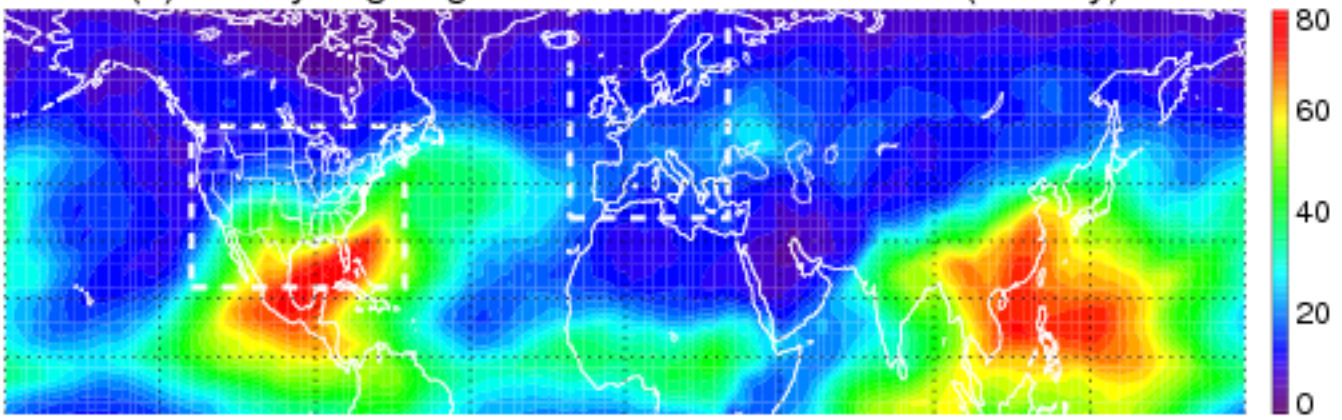

(b) 10-day Lagrangian TROP Strat. Influence (%)

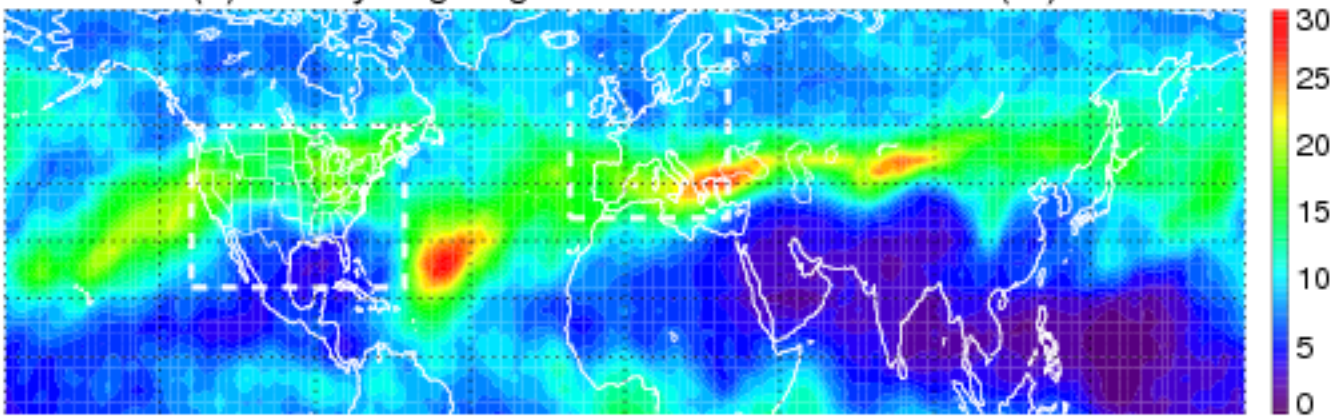

(c) 10-day Lagrangian TROP PBL Influence (%)

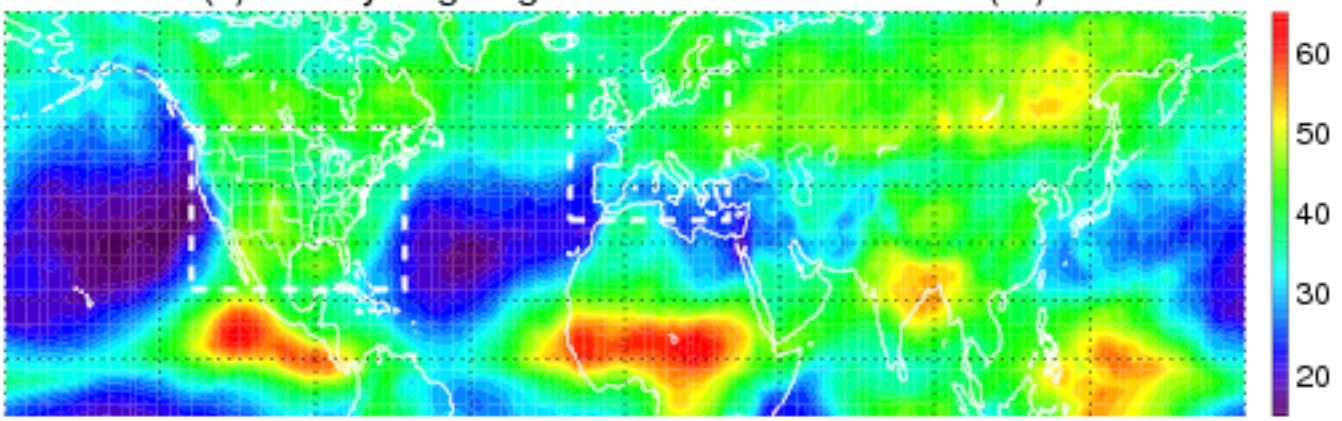

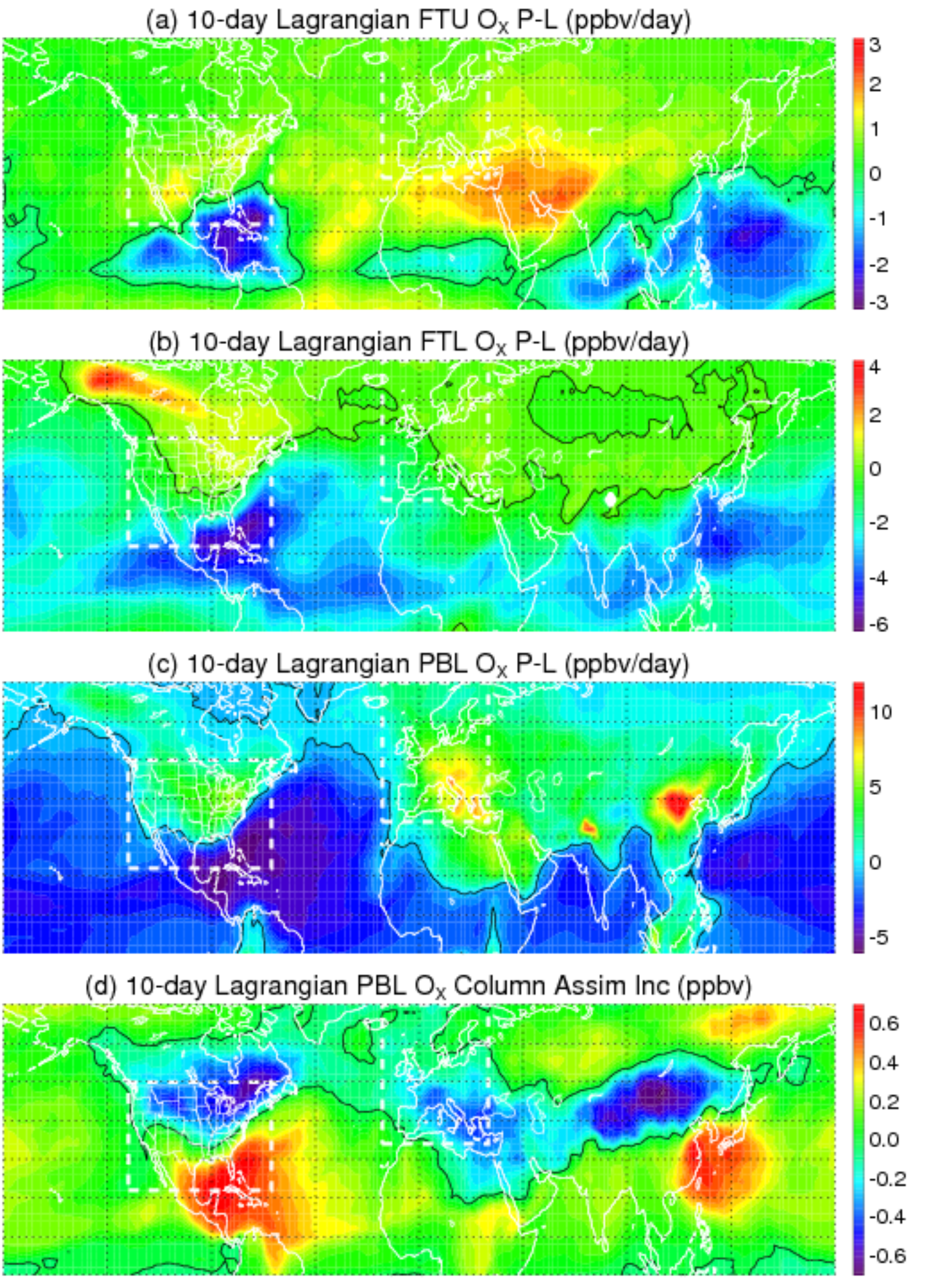
(a) 10-day Lagrangian FTU O_X P-L (ppbv/day)
3
2
1
0
-1
-2
-3
(b) 10-day Lagrangian FTL O_X P-L (ppbv/day)
4
2
0
-2
-4
-6
(c) 10-day Lagrangian PBL O_X P-L (ppbv/day)
10
5
0
-5
(d) 10-day Lagrangian PBL O_X Column Assim Inc (ppbv)
0.6
0.4
0.2
0.0
-0.2
-0.4
-0.6

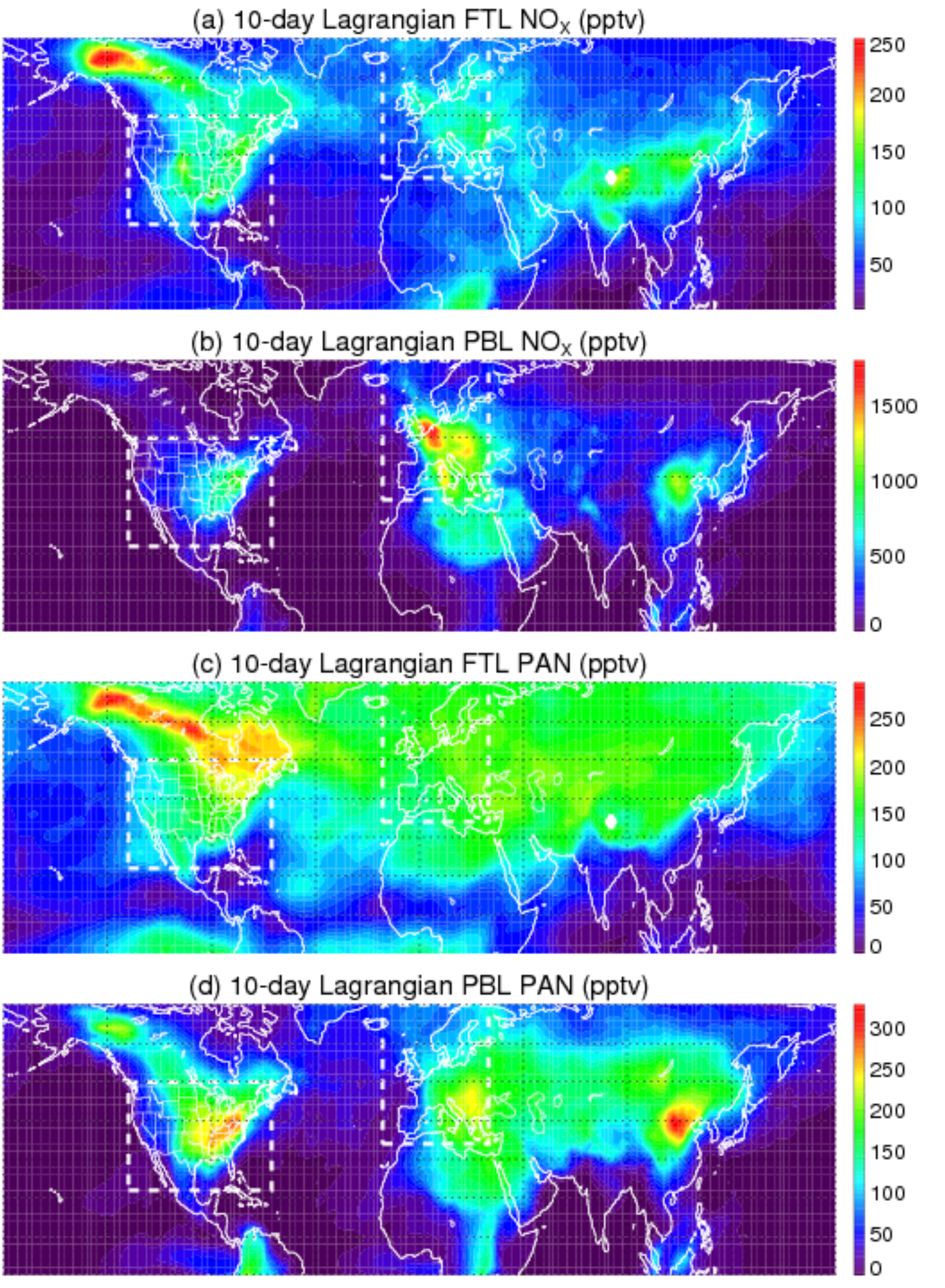
(a) 10-day Lagrangian FTL NO_X (pptv)
250
200
150
100
50
(b) 10-day Lagrangian PBL NO_X (pptv)
1500
1000
500
0
(c) 10-day Lagrangian FTL PAN (pptv)
250
200
150
100
50
0
(d) 10-day Lagrangian PBL PAN (pptv)
300
250
200
150
100
50
0

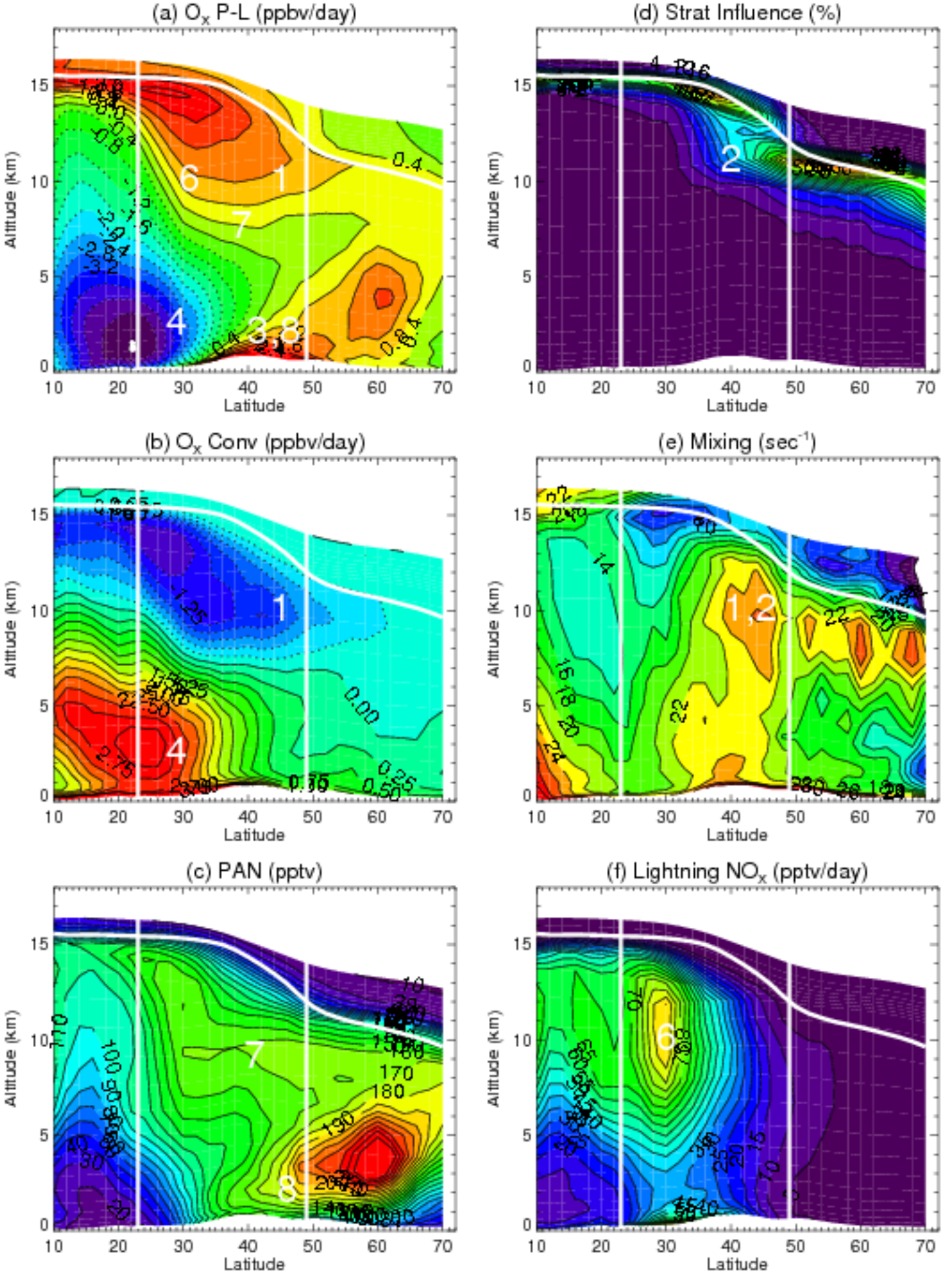
(a) O_x P-L (ppbv/day)
(d) Strat Influence (%)
(b) O_x Conv (ppbv/day)
(e) Mixing (sec^{-1})
(c) PAN (pptv)
(f) Lightning NO_x (pptv/day)
Altitude (km)
Latitude
0
5
10
15
10
20
30
40
50
60
70
1
2
3
4
6
7
8
1,2

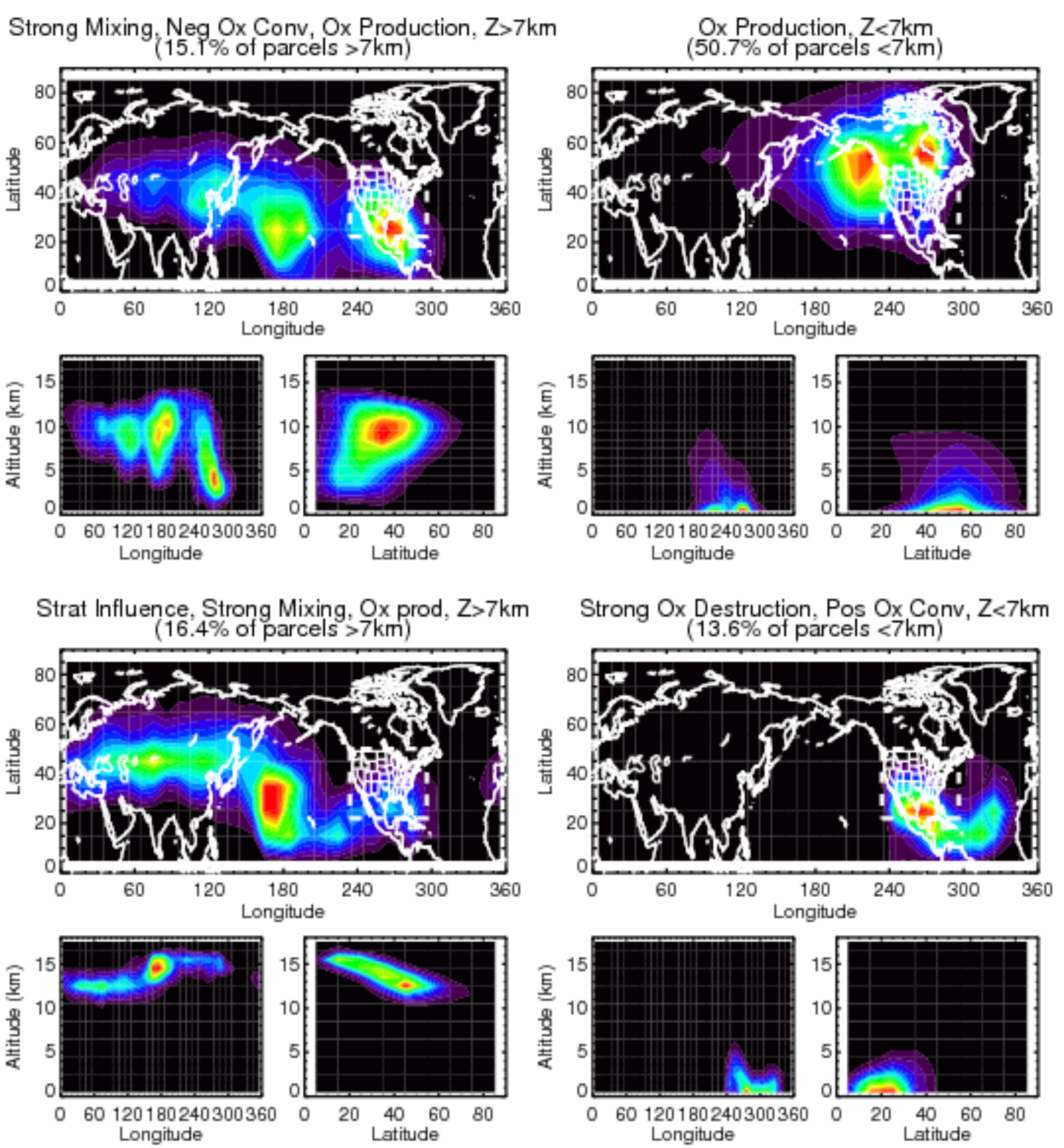
Strong Mixing, Neg Ox Conv, Ox Production, Z>7km
(15.1% of parcels >7km)
Ox Production, Z<7km
(50.7% of parcels <7km)
Strat Influence, Strong Mixing, Ox prod, Z>7km
(16.4% of parcels >7km)
Strong Ox Destruction, Pos Ox Conv, Z<7km
(13.6% of parcels <7km)
Latitude
Longitude
Altitude (km)

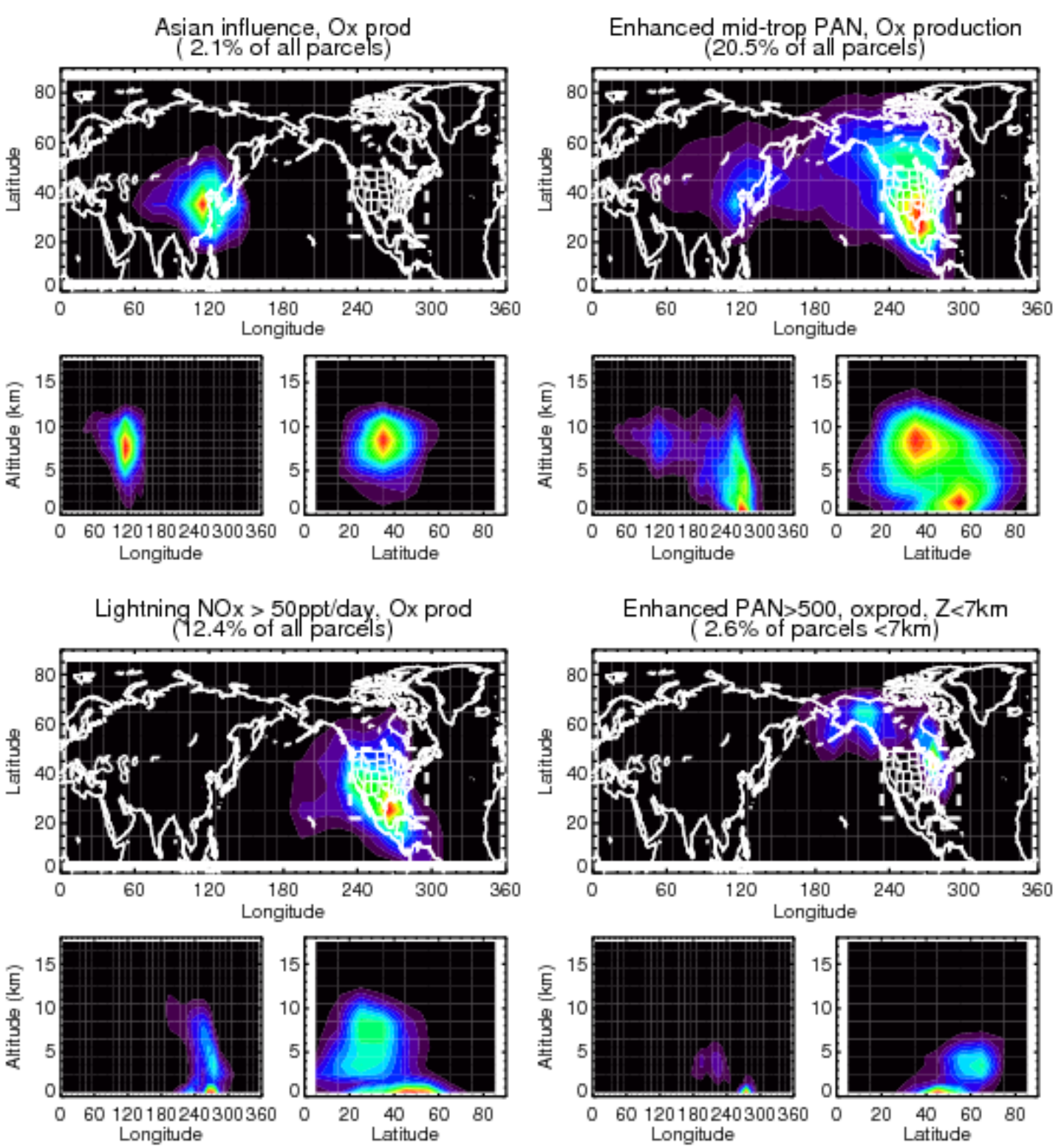
Asian influence, Ox prod
(2.1% of all parcels)
Enhanced mid-trop PAN, Ox production
(20.5% of all parcels)
Lightning NOx > 50ppt/day, Ox prod
(12.4% of all parcels)
Enhanced PAN>500, oxprod, Z<7km
(2.6% of parcels <7km)
Latitude
Longitude
Altitude (km)
0 60 120 180 240 300 360
0 20 40 60 80
0 5 10 15 20 40 60 80

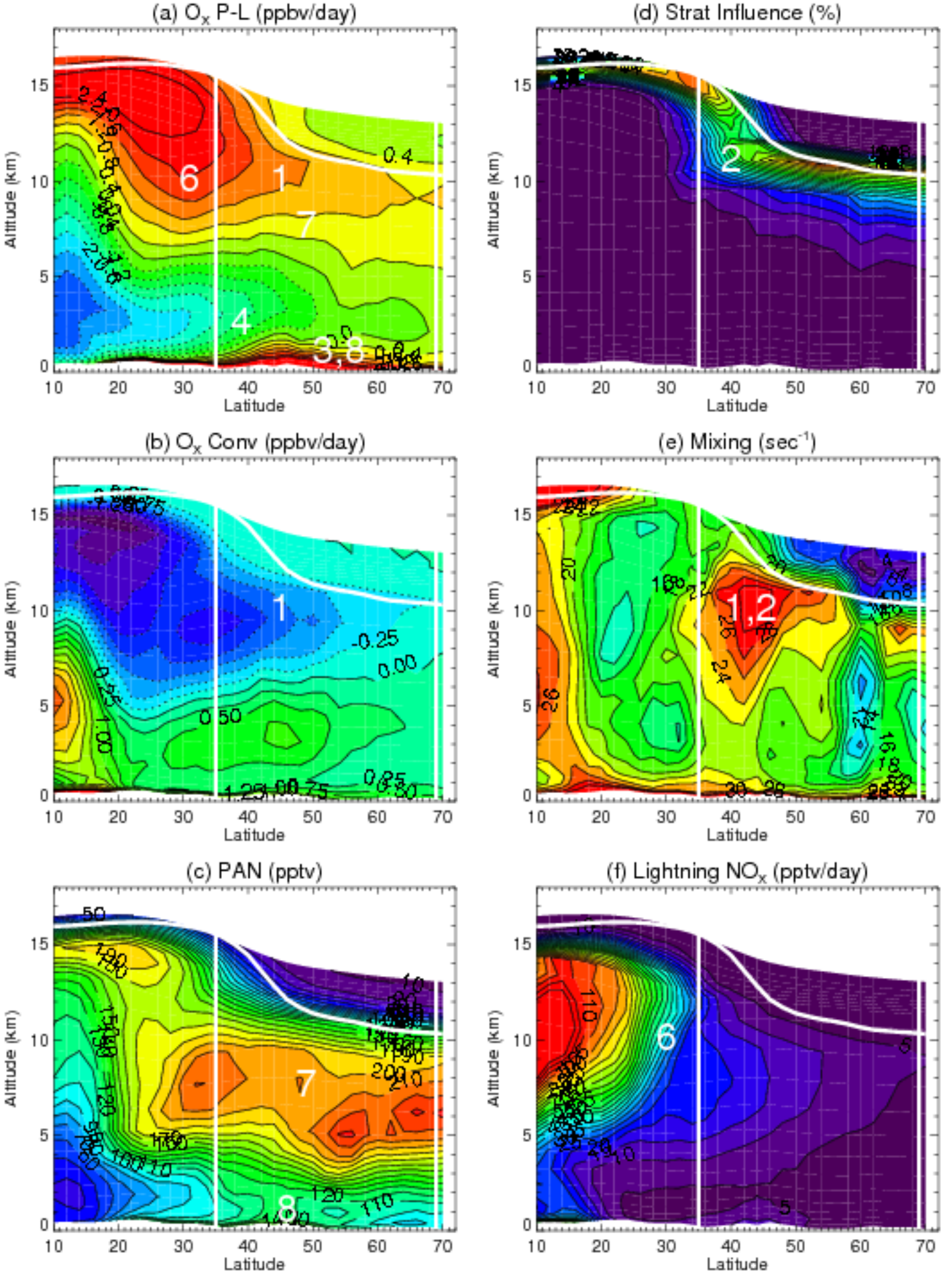
(a) O_x P-L (ppbv/day)
(d) Strat Influence (%)
(b) O_x Conv (ppbv/day)
(e) Mixing (sec^{-1})
(c) PAN (pptv)
(f) Lightning NO_x (pptv/day)
Altitude (km)
Latitude

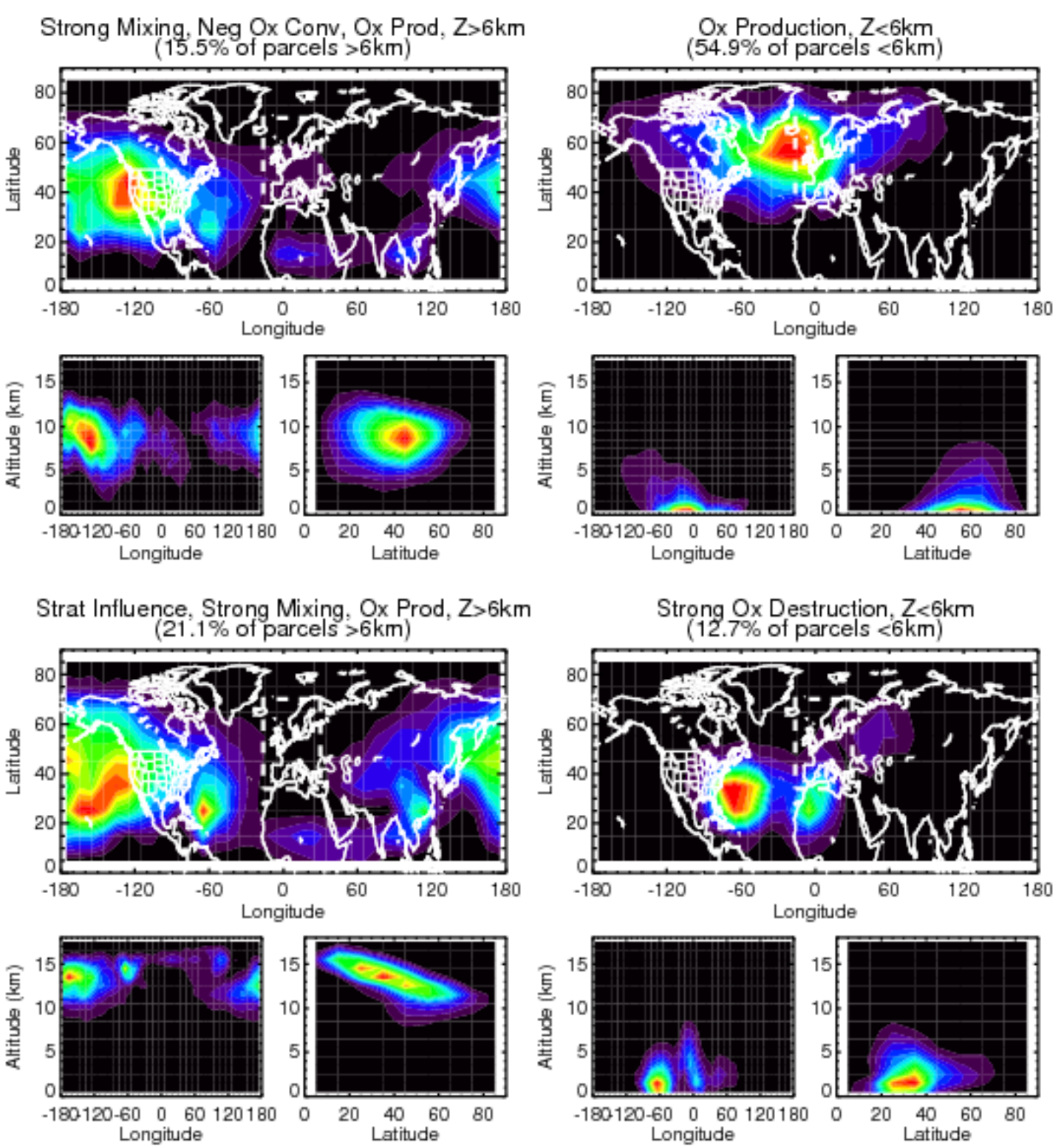
Strong Mixing, Neg Ox Conv, Ox Prod, Z>6km
(15.5% of parcels >6km)
Ox Production, Z<6km
(54.9% of parcels <6km)
Strat Influence, Strong Mixing, Ox Prod, Z>6km
(21.1% of parcels >6km)
Strong Ox Destruction, Z<6km
(12.7% of parcels <6km)
Latitude
Longitude
Altitude (km)

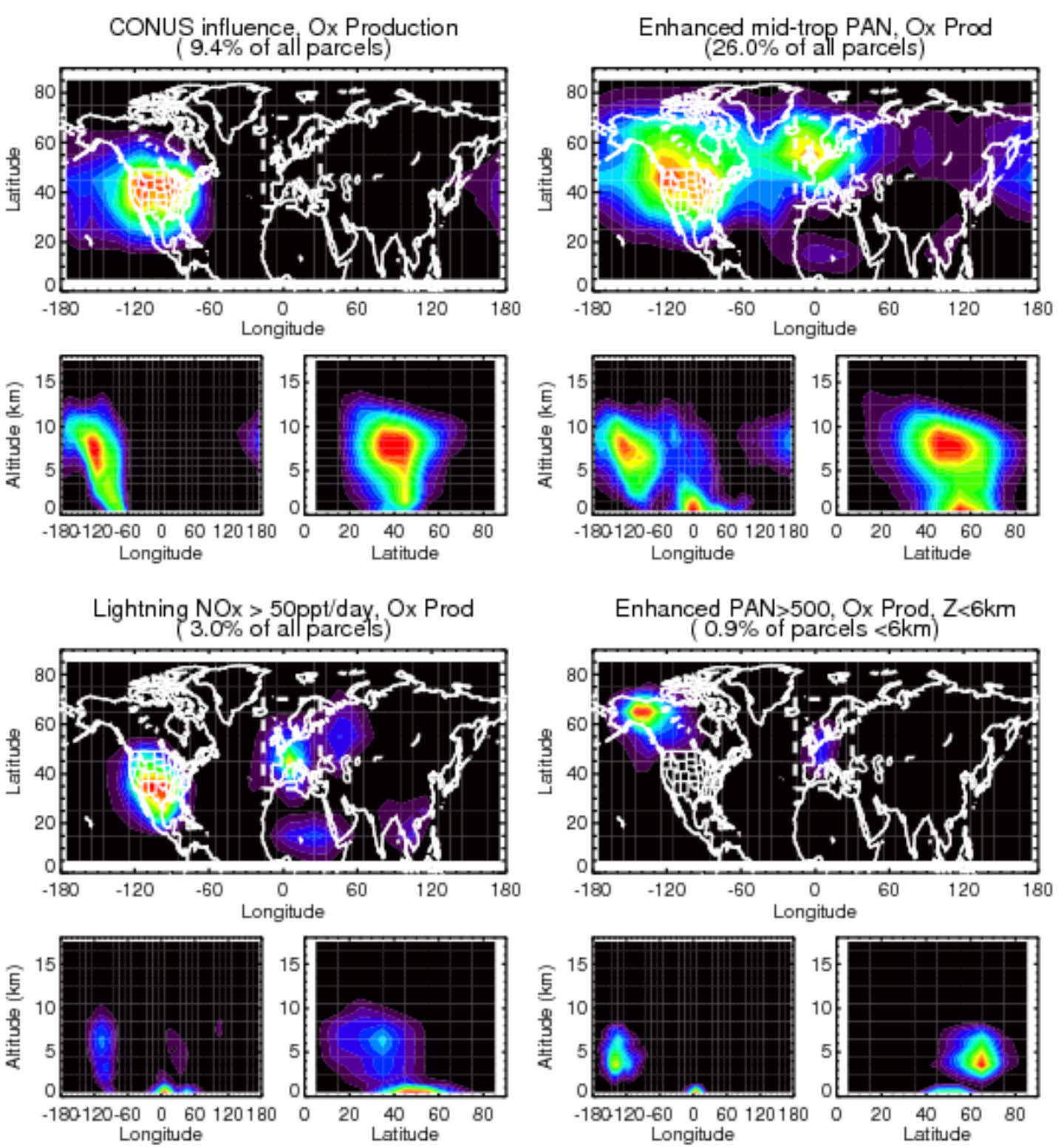
CONUS influence, Ox Production
(9.4% of all parcels)
Enhanced mid-trop PAN, Ox Prod
(26.0% of all parcels)
Lightning NOx > 50ppt/day, Ox Prod
(3.0% of all parcels)
Enhanced PAN>500, Ox Prod, Z<6km
(0.9% of parcels <6km)
Latitude
Longitude
Altitude (km)